Journal of Materials Chemistry C

Accepted Manuscript

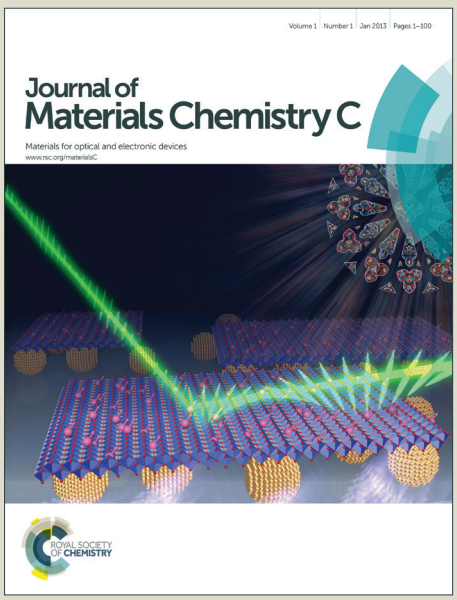

ROYAL SOCIETY OF CHEMISTRY

www.rsc.org/materialsC

Simultaneous achievement of low efficiency roll-off and stable color in highly efficient single-emitting-layer phosphorescent white organic light-emitting diodes

Baiquan Liu [a)] Lei Wang [a)] Miao Xu [a)] Hong Tao [a)] Xingheng Xia [a)] Jianhua Zou [a)*]

Yueju Su [b)] Dongyu Gao [b)] Linfeng Lan [a)] Junbiao Peng [a)*]

[a] Institute of Polymer Optoelectronic Materials and Devices, State Key Laboratory of Luminescent Materials and Devices, South China University of Technology, Guangzhou 510640, China

[b] New Vision Opto-Electronic Technology Co., Ltd, Guangzhou 510530, China

Abstract: A highly efficient single-emitting-layer white organic light-emitting diode with low efficiency roll-off and great color-stability has been fabricated and characterized. The resulting device achieves a forward-viewing current efficiency of 45.2 cd/A and a power efficiency of 37.1 lm/W at a luminance of 100 cd/m^2. Even at 1000 cd/m^2, a current efficiency of 43.6 cd/A and a power efficiency of 31.3 lm/W can be obtained, indicating that the device exhibits low efficiency roll-off. Besides, only a slight color-shift $\Delta\leq$ (0.025, 0.006) can be observed during a large range of luminance, revealing that the device shows stable color. It is found that such superior properties are originated from the introduction of multifunctional dopants as well as the bipolar host. Moreover, it is demonstrated that the dopants with low concentrations have almost no influence on the electrical property when negligible energy barriers exist between the dopants and charge transport layers.

Keywords: white organic light-emitting diodes, efficiency, stable color, roll-off.

1. Introduction

White organic light-emitting diodes (WOLEDs) are now entering the mainstream display markets and also being intensively explored for the next generation solid-state lighting applications owing to their high efficiency, flexibility, light weight and low cost [1]. Since phosphorescent emitters allow for a conversion of up to 100% of injected charges into emitted photons (both singlet and triplet excitons can be harvested), leading to a theoretical internal quantum efficiency of unity [2], highly efficient phosphorescent materials are generally imperative to boost the efficiency of WOLEDs. In order to generate the desired white emission, mixtures of the three primary colors (red, green and blue) or two complementary colors, for example, blue and yellow, are typically required, and various approaches towards realizing WOLEDs have been reported [2-4]. Among these approaches, the two or multiple emitting layer (EML) structures are widely adopted in WOLEDs, which inevitably result in higher complexity, time-consuming, control difficulties, higher operational voltages as well as higher cost [3, 4].

To address the above-mentioned issues, elaborate device structures and elegant materials have to be developed. In terms of device structures, single-EML WOLEDs based on a versatile host doped with different color dopants [5, 6], are of particular interest, since they can offer some unique advantages, such as simplified structures and more cost-effective fabrication processes. In fact, a large number of endeavors have been made via this simple way [5, 6]. For example, Wang et al. used a hole-type host 4,4',4''tri(*N*-carbazolyl)triphenylamine (TCTA) to achieve a high-efficiency

single-EML WOLED (33.0 lm/W at a low current density) [5a]. They also utilized the host 1,3-bis(9-carbazolyl)benzene (mCP) to obtain a white device with a forward-viewing power efficiency (PE) of 42.5 lm/W at a low luminance and 19 lm/W at 500 cd/m^2 [5b]. However, it is easily noted that these WOLEDs with unipolar hosts usually suffer serious efficiency roll-off and unstable color [5]. This is because the unbalanced charge carriers of unipolar hosts, which mainly transport holes or electrons, frequently cause the charge recombination near the hole transport layer (HTL) or electron transport layer (ETL), leading to a narrow recombination zone and further possible triplet-triplet annihilation (TTA) and exciton diffusion [4a]. To alleviate these difficulties, a more advantageous approach may be the use of bipolar hosts to realize single-EML WOLEDs. Since bipolar hosts can transport both holes and electrons, balanced charge fluxes and wide recombination zones can be provided [6], developing WOLEDs with high-efficiency, low efficiency roll-off and better color-stability. For example, Ho et al. synthesized a carbazole-based coplanar molecule (CmInF) as the bipolar host, achieving a single-EML WOLED with an efficiency of 11.2 lm/W [6a]. Hung et al. fabricated dual-emitter WOLEDs with a co-doped single-EML, exhibiting a satisfactory efficiency (17 lm/W) and a stable color [6b]. Gong et al. realized a highly efficient single-EML device (42.7 lm/W at ~30 cd/m^2 and 25.2 lm/W at 1000 cd/m^2) by using a silicon-bridged molecule as the bipolar host [6c]. Yang et al. modified 4,4′,4″-Tri(N-carbazolyl)triphenylamine as a bipolar host for highly efficient single-EML WOLED, achieving a maximum efficiency of 47 lm/W at a low brightness and 20 lm/W at 1000 cd/m^2. Based on these

facts, it can be concluded that the utilization of single-EML structure is a very promising and simple way to construct efficient WOLEDs. Although the efficiency of single-EML WOLEDs has experienced step-by-step increase over the past years and already exceeded some of the best multi-EML structures, highly efficient phosphorescent single-EML WOLEDs with low efficiency roll-off and stable color are still rather scare, indicating that there is much room to further enhance the performance of phosphorescent WOLEDs by using this simplified architecture. Moreover, the color-stability of single-EML WOLEDs is negligibly reported and no work has been documented to study the effect of dopants on the color-stability in single-EML WOLEDs.

In this paper, we have developed a highly efficient single-EML WOLED with a bipolar host, achieving low efficiency roll-off and stable color. At 100 cd/m^2, the forward-viewing current efficiency (CE) and PE of the resulting device are 45.2 cd/A and 37.1 lm/W, respectively. At 1000 cd/m^2, the CE is still retained at 43.6 cd/A while the PE is as high as 31.3 lm/W. To our knowledge, the efficiencies are one of the highest levels for the reported WOLEDs in the literature so far [1-6]. Besides, the resulting device exhibits a stable color during a large range of luminance from 10 cd/m^2 to 12000 cd/m^2. Encouraged by the superior properties, the origin of the color-stability and reduced efficiency roll-off is comprehensively investigated. The high performances are attributed to the utilization of multifunctional guests which can lead to the recombination ratio in the EML constant with increasing current coupled with the use of the bipolar host which can result in balanced charge fluxes and a broad

distribution of recombination region within the EML. Besides, it is found that the dopants with low concentrations have almost no influence on the electrical property when there are negligible energy barriers between the dopants and charge transport layers.

2, Experimental

Figure 1 depicts the studied WOLEDs. The resulting WOLED has the configuration of ITO/MeO-TPD : F4-TCNQ (100 nm, 4%)/TAPC (20 nm)/ 26DCzPPy : FIrpic : $(MPPZ)_2Ir(acac)$ (8 nm, 1: 25%: 1%)/TmPyPB (45 nm)/LiF (1 nm)/Al (200 nm), where ITO is indium tin oxide, MeO-TPD is N, N, N',N'-tetrakis(4-methoxyphenyl)-benzidine, F4-TCNQ is tetrafluoro-tetracyanoqino dimethane, TAPC is 1-bis[4-[N,N-di(4-tolyl)amino]phenyl]-cyclohexane, TmPyPB is 1,3,5-tri(*m*-pyrid-3-yl-phenyl)benzene, the sky blue material iridium(III)bis[(4,6-difluo-rophenyl)-pyridinato-N,C2] (Firpic) and orange material iridium (III) diazine complexes $(MPPZ)_2Ir(acac)$, codoped into 2,6-bis(3-(carbazol-9-yl)phenyl)pyridine (26DCzPPy) host to achieve balanced white light. The ITO surface was cleaned by using ultrasonicwater for 3 minutes and then dried at 80 □ for 20 minutes before it was loaded into an evaporator, and then 100 nm thick MeO-TPD: F4-TCNQ (as a hole injection layer (HIL)), 20 nm thick TAPC(as a HTL), 8 nm thick 26DCzPPy : FIrpic : $(MPPZ)_2Ir(acac)$ (as an EML), 45 nm thick TmPyPB (as an ETL), and finally 1 nm thick LiF and 200 nm thick Al cathode were evaporated in sequence. All material layers were thermally deposited without breaking the vacuum at a base pressure of 2×10^{-7} Torr. In the deposition of the

doping layers, deposition rates of both host and guest were controlled with their correspondingly independent quartz crystal oscillators. The devices were encapsulated immediately after preparation under a nitrogen atmosphere using epoxy glue and glass lids. The electroluminescent (EL) spectra, Commission International de I'Eclairage (CIE) color coordinates and color rendering index (CRI) of packaged devices were obtained by a Konica Minolta CS2000 spectra system. The emission area of the devices is 3×3 mm^2 as defined by the overlapping area of the anode and cathode. The luminance-current density (J) -voltage (V) characteristics were recorded simultaneously, using a computer-controlled source meter (Keithley 2400) and multimeter (Keithley 2000) with a calibrated silicon photodiode. All the measurements were carried out at room temperature under ambient conditions.

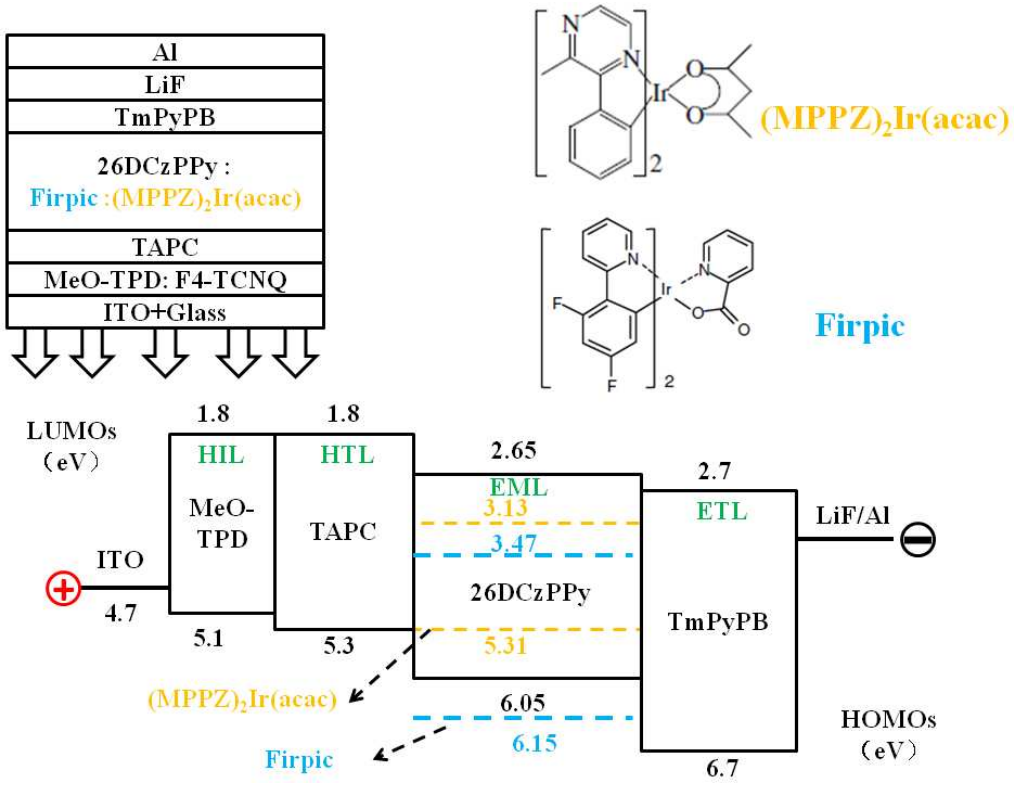

Figure. 1. Top: The schematic layer structure of processed WOLED and the chemical

structure of emissive dopants. Bottom: Proposed energy-level diagram of the WOLED, showing the highest occupied and lowest unoccupied molecular orbital energies relative to the vacuum level.

3. Results and discussions

Since the improvement of both efficiency and stability in WOLEDs can be expected with rational design of structures, several strategies are employed to achieve high efficiency, low efficiency roll-off together with stable EL spectra for the simplified WOLED.

First, to lower manufacturing cost, device architectures should be uncomplicated. Thus, we utilized two complementary colors to give off white emission, surprisingly, performances of the simple device are very impressive.

Second, to maximize exciton formation and emission in WOLEDs, it is necessary to optimize the dopant concentration in the host-guest system. Therefore, devices with various concentrations of dopant were tested to determine the best concentrations. As the results showed in our lab, it was found that the optimized concentrations for the blue guest Firpic and orange dopant $(MPPZ)_2Ir(acac)$ were fixed at 25% and 1%, respectively. It should be pointed out that the concentration of $(MPPZ)_2Ir(acac)$ should be low, or else no balanced white emission can be observed. This is because the orange emission occurred from the combined effects of efficient energy transfer from the blue phosphor and exciton formation by direct charge trapping on $(MPPZ)_2Ir(acac)$ dopant [5c, 6b].

Next, it is noted that the 26DCzPPy host has a great effect on the device

performance. On the one hand, the triplet energy of the host material 26DCzPPy is high enough (2.71 eV) [7] to satisfy the blue Firpic guest (2.65 eV) [7], or the orange $(MPPZ)_2Ir(acac)$ emitter (< 2.2 eV) [8], preventing reverse energy transfer from the dopants to the host as well as confining triplet excitons in the EML, which enables consumption of the electrically generated triplets contributing to emission [7a]. On the other hand, both the hole mobility and electron mobility of 26DCzPPy are ~10^{-5} $cm^2/(V\ s)$ [7b], implying that 26DCzPPy have decent and balanced charge carrier transport properties for the hole-electron recombination process and confinement of the exciton formation zone in the EML. As a matter of fact, the bipolar charge-transporting property of 26DCzPPy is also expected to broaden the excitons recombination zone, which can effectively improve the device efficiency and reduce the efficiency roll-off [6c]. Besides, the highest occupied molecular orbital (HOMO) and the lowest unoccupied molecular orbital (LUMO) of the 26DCzPPy are 2.65 eV and 6.05 eV [7b], respectively, which matches well with those of neighboring active layers to reduce the hole and electron injection barrier, thus lowering the device driving voltages.

In addition, the charge transport layers play key roles in guaranteeing the device performance. On the one hand, the electron mobility of TmPyPB is as high as 10^{-3} $cm^2/(V\ s)$ [9], which can give an effective electron injection and thus an improved carrier balance [1c]. Besides, TmPyPB can effectively block holes and confine excitons in the emissive zone because of its deep HOMO of 6.7 eV [9] and high triplet energy of 2.75 eV [9]. The large energy offset (0.65 eV) of the HOMO between

TmPyPB and 26DCzPPy (or 0.55 eV between TmPyPB and Firpic) effectively prevents holes from transporting into the adjacent ETL. As a result, holes are well confined in the EML. On the other hand, the TAPC HTL exhibits a high hole mobility (10^{-2} $cm^2/(V\ s)$) [10a], high triplet energy (2.87 eV) [10a, 10b], coupled with a large difference in LUMO levels between TAPC and 26DCzPPy (0.85 eV) [10a, 10c] which greatly reduces the electron leakage from the EML [1c]. Thus, both charges and generated excitons are expected to be well confined within the EML due to the effect of charge transport layers, enhancing the device performance [5a].

Finally, the use of thin EML has been previously demonstrated to be an effective way to lower operational voltages, thus improving efficiency and lowering color shift [3a]. Herein, we selected 8 nm thick EML for this purpose.

Based on the above considerations, we put forward a simple WOLED with single-EML structure (named as W_1), simultaneously achieving high efficiency, low efficiency roll-off and stable color. The CE and PE of the resulting device (W_1) in dependence of the luminance are shown in figure 2. It is seen that at a luminance of 100 cd/m^2, the forward-viewing CE and PE of W_1 are 45.2 cd/A and 37.1 lm/W, respectively. Remarkably, W_1 exhibits a significantly reduced efficiency roll-off, the CE is still retained at 43.6 cd/A while the PE is as high as 31.3 lm/W at the illumination-relevant luminance of 1000 cd/m^2. Compared with the conventional phosphorescent WOLEDs, which usually exhibit a tremendous efficiency roll-off at high luminance, our device can effectively solve this notorious roll-off problem. Since illumination sources are typically characterized by their total emitted power [5b], the

total PE of W_1 is 63.1 lm/W at 100 cd/m^2, which slightly rolls off to 53.2 lm/W at 1000 cd/m^2. To the best of our knowledge, the efficiency (53.2 lm/W) represents the highest value in the single-EML WOLEDs with bipolar hosts at the practical luminance. Moreover, it is noted that much higher efficiency can be obtained if we replaced the TmPyPB with an n-doped ETL to form a p-i-n structure [3d] or enhanced the light extraction by using out-coupling methods, including microlens [3d] and sandblasting techniques, as demonstrated in our previous report [11].

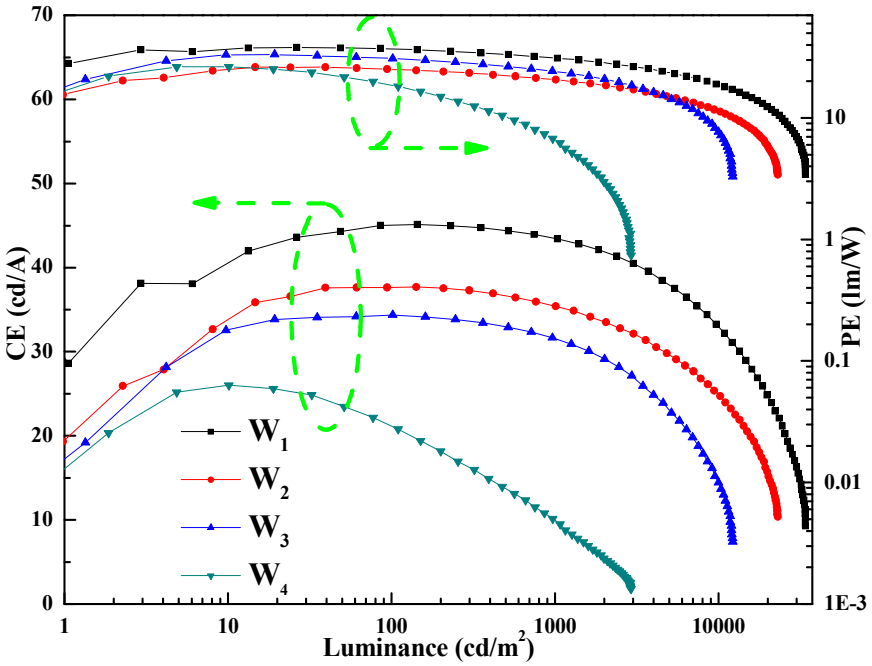

Figure. 2. Power and current efficiencies as a function of luminance for W_1~W_4.

Spectral stability upon change of luminance was also studied, a blue emission peak at 473 nm (with a shoulder at 499 nm) and an orange emission at 567 nm are clearly displayed in figure 3, covering all wavelengths from 380 nm to 780 nm. Remarkably, when the luminance increases from 10 cd/m^2 to 12000 cd/m^2, the CIE coordinates of the device only experience a negligible change from (0.390, 0.454) to

(0.365, 0.448). The little color-shift may originate from the shift of recombination zone with increasing voltage and easier formation of high energy excitons at higher voltage [12]. The total CIE coordinates variation is $\Delta(x, y) \leq (0.025, 0.006)$, revealing that W_1 exhibits one of the most stable color in phosphorescent WOLEDs in the literature until now [4-6].

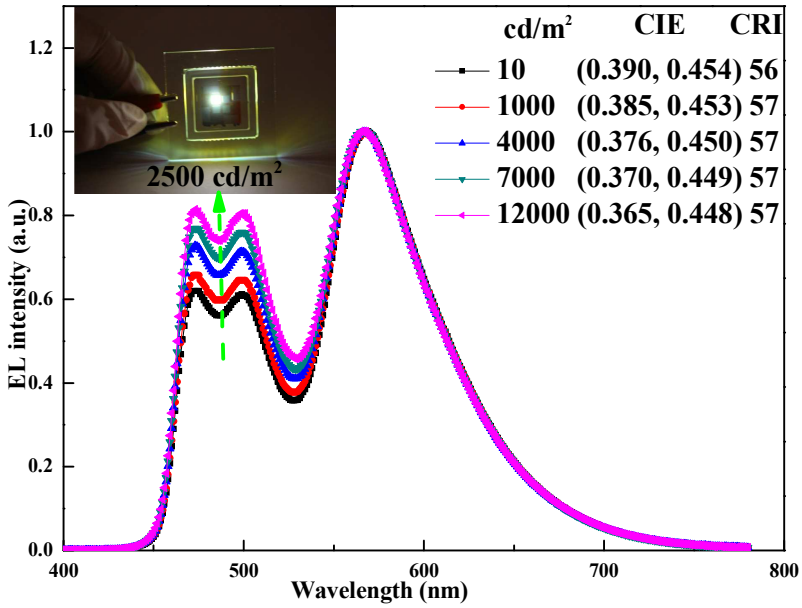

Figure. 3. Normalized EL spectra of W_1 at various luminances. Affected by the two-color system, the CRI of the WOLED is not high (57 at 1000 cd/m^2).

Encouraged by the outstanding results obtained from the single-EML WOLED, we subsequently performed a comprehensive study to unveil the origin of stable color and reduced efficiency roll-off.

In general, the reduction of charge mobility associated with host-dopant energy level difference leads to the recombination ratio being constant in the EML, thus greatly stabilizing the EL spectrum [1c, 4b, 13]. To clarify the effect of phosphors-doped 26DCzPPy on electrical properties, the hole-only and electron-only

devices were fabricated with the configurations of ITO/MeO-TPD : F4-TCNQ (100 nm, 4%)/TAPC (20 nm)/ 26DCzPPy : dopants (8 nm)/TAPC(20 nm)/Al (200 nm) and ITO/LiF (1nm)/TmPyPB (45 nm)/26DCzPPy : dopants (8 nm)/ TmPyPB (45 nm)/LiF (1 nm)/Al (200 nm), respectively, where dopants denote none for device H_1 and E_1, 25% Firpic for device H_2 and E_2, 1% $(MPPZ)_2Ir(acac)$ for device H_{31} and E_{31}, 25% Firpic and 1% $(MPPZ)_2Ir(acac)$ codoped for device H_{41} and E_{41}. As depicted in figure 4, the hole-only and electron-only J-V curves of Firpic or/and $(MPPZ)_2Ir(acac)$-doped 26DCzPPy exhibit dramatic changes. Comparing device H_2 with H_1, the hole-only J decreases rapidly upon doping Firpic into 26DCzPPy. Since Firpic has the HOMO of 6.15 eV [7b] which is 0.1 eV deeper than that of 26DCzPPy, the injected holes may collide with the positive barriers and be scattered by these barriers, leading to a reduction of the drift velocity due to an increase of the total transit path [4b]. As a result, the hole mobility is reduced upon doping Firpic into the device. However, the addition of $(MPPZ)_2Ir(acac)$ shows nearly no influence on the hole injection and transport in 26DCzPPy since the J of H_{31} is similar to that of H_1, which can be understood as follows. From figure 1, we infer a high barrier to hole injection into 26DCzPPy from TAPC of 0.75 eV, while hole injection into $(MPPZ)_2Ir(acac)$ is energetically favorable with only a 0.01 eV barrier because the HOMO of this guest is 5.31 eV [8]. As a result, holes may be easily injected into the EML and the J of H_{31} can be increased much by virtue of the $(MPPZ)_2Ir(acac)$ dopant. However, only contradict results are observed. In fact, this phenomenon is attributed to the quite low concentration of this dopant (1%) which has a negligible influence on the hole

transport characteristic of the device [7b]. This analysis is evidently confirmed when making a comparison between device H_2 and H_{41}, it is clear seen that the addition of $(MPPZ)_2Ir(acac)$ also shows almost no effect on the hole injection/transport in the 26DCzPPy : Firpic system, as shown in figure 4. Whereas, upon doping the Firpic or/and $(MPPZ)_2Ir(acac)$ into the 26DCzPPy host, the J of electron-only devices decreases rapidly, which is attributed to the electron trapping effects of dopants [1c]. The LUMO level of Firpic (3.47 eV) [7] is much lower than that of 26DCzPPy (2.65 eV) [7], resulting in electrons being easily trapped by Firpic [1c]. Although Firpic is a well-known electron-type dopant [3a], the electron trapping effect by the Firpic reduces the electron transport of device E_2 compared with that of device E_1. Moreover, the electron trapping effect can also occur in $(MPPZ)_2Ir(acac)$ owing to its low LUMO (3.13 eV) [8]. Therefore, it is reasonable that device E_{41} exhibits the lowest J among the electron-only devices. As a result, the mobilities of both holes and electrons are reduced upon doping Firpic or/and $(MPPZ)_2Ir(acac)$ into this device, leading to the recombination ratio in the EML being constant with increasing current, which is beneficial to getting high color-stability and low efficiency roll-off [13].

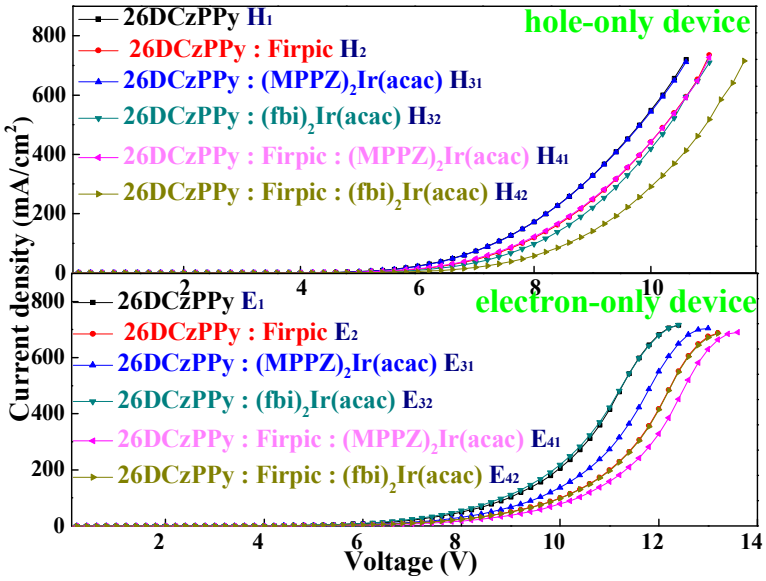

Figure. 4. J–V curves of single-carrier transporting devices based on Firpic, $(MPPZ)_2Ir(acac)$ and $(fbi)_2Ir(acac)$-doped 26DCzPPy.

To further demonstrate the significance of the orange dopant $(MPPZ)_2Ir(acac)$ in making a contribution to maintaining the color constancy and achieving high efficiency in the WOLED, another device (W_2) was fabricated by replacing this orange dopant with bis(2-(9,9-diethyl-9H-fluoren-2-yl)-1-phenyl-1Hbenzoimidazole-N,C^3)iridium(acetylacetonate) ($(fbi)_2Ir(acac)$). The configuration of W_2 is ITO/MeO-TPD : F4-TCNQ (100 nm, 4%)/TAPC (20 nm)/ 26DCzPPy : Firpic : $(fbi)_2Ir(acac)$ (8 nm, 1: 25%: 1%)/TmPyPB (45 nm)/LiF (1 nm)/Al (200 nm). The device structure and EL spectra at various luminances are shown in figure 5. The total CIE coordinates variation of $(fbi)_2Ir(acac)$ based device is $\Delta(x, y) \leq (0.062, 0.022)$ as the luminance increases from 10 cd/m^2 to 12000 cd/m^2, which is nearly three times larger than that of W_1. Besides, the efficiency of W_2 is lower than that of W_1, as shown in figure 2 and table 1. These

facts evidently demonstrate that the introduced orange $(MPPZ)_2Ir(acac)$ dopant is significant to achieving the high performance in the resulting WOLED (W_1).

We also fabricated the hole-only and electron-only devices to deeply investigate the effect of $(fbi)_2Ir(acac)$-doped 26DCzPPy on electrical properties with the configurations of ITO/MeO-TPD : F4-TCNQ (100 nm, 4%)/TAPC (20 nm)/ 26DCzPPy : dopants (8 nm)/TAPC(20 nm)/Al (200 nm) and ITO/LiF(1nm)/TmPyPB(45 nm)/26DCzPPy : dopants (8 nm)/ TmPyPB (45 nm)/LiF (1 nm)/Al (200 nm), respectively, where dopants denote 1% $(fbi)_2Ir(acac)$ for device H_{32} and E_{32}, 25% Firpic and 1% $(fbi)_2Ir(acac)$ codoped for device H_{42} and E_{42}. Since the HOMO of $(fbi)_2Ir(acac)$ is 5.1 eV [5b] which is higher than that of 26DCzPPy (6.05 eV) [8], holes being easily trapped by $(fbi)_2Ir(acac)$ [1c]. Hence, the J of H_{32} with the $(fbi)_2Ir(acac)$ dopant is lower than that of both H_1 without dopants and H_{31} with the $(MPPZ)_2Ir(acac)$ dopant. As a result, it is reasonable that device H_{42} exhibits the lowest J among the hole-only devices due to the effect of $(fbi)_2Ir(acac)$ and Firpic dopant, as shown in figure 4. On the other hand, the addition of $(fbi)_2Ir(acac)$ dopant has negligible influence on the electron injection/transport in the 26DCzPPy host and 26DCzPPy : Firpic system since the J of E_{32} and E_{42} is similar to that of E_1 and E_2, respectively, as shown in figure 4. This phenomenon can also be attributed to the low concentration of $(fbi)_2Ir(acac)$ dopant (1%) in the device [7b], similar to the above demonstrated fact that the low concentration of $(MPPZ)_2Ir(acac)$ dopant has negligible effect on the hole injection and transport. Although the LUMO of $(fbi)_2Ir(acac)$ is 2.7 eV [5b] which is the same as that of TmPyPB, electrons may

inject resonantly into the $(fbi)_2Ir(acac)$ LUMO from TmPyPB LUMO and transport by hopping on dopant sites, leading to the enhancement of electron current [14]. However, the low concentration of this dopant results in a negligible influence on the electron transport characteristic of the device [7b]. Recently, Zhao et al. found that the hole transport is not affected by the dopant when there is a same HOMO level between the dopant and the host as the dopant concentration is low (5%) [15a]. While Baek et al. proposed an idea that the dopant with 4% concentration has little effect on the electron conduction properties of the host when their LUMO levels are almost the same [15b]. Herein, we have evidently demonstrated that the dopants with low concentrations have almost no effect on the electrical property when there are negligible energy barriers between the dopants and charge transport layers, considering the similar J of H_1 and H_{31} or similar J of H_2 and H_{41} in the hole-only devices or the similar J of E_1 and E_{32} or similar J of E_2 and E_{42} in the electron-only devices, as shown in figure 4. Since it is well-known that fine-tuning the charges, which are associated with the internal physical processes within the device, is usually the key core to ultimately furnish efficient white light, careful management of charges is undoubtedly being one of crucial factors in realizing high-performance WOLEDs, regardless of whatever device structures and endeavors the researchers create [1c]. Therefore, it is beyond doubt that our demonstrated results will be beneficial to the rational design of both material and device structure for high-performance WOLEDs. Particularly, a large number of issues can be effectively manipulated by virtue of the above obtained results that the dopants can play multifunctional roles in the device

performance, such as management of charge balance, singlets and triplets harnessing, control of recombination zone, exciton generation, adjusting charge or exciton diffusion, effective host (guest)-to-guest mutual energy transfer, confinement of excitons, etc.

From figure 1, it is noted that a large energy barrier (0.75 eV) exists between the HOMO of TAPC and 26DCzPPy, while only a slight energy barrier (0.15 eV) exists between the LUMO of TmPyPB and 26DCzPPy, which indicates electrons are much easier than holes can be injected into the EML due to the fact that the current flow is limited by the injection of carriers when the injection energy barrier is higher than 0.3-0.4 eV [16]. In the case of W_2, the $(fbi)_2Ir(acac)$ dopant reduces the hole mobility but has almost no effect on the electron transport, which leads to holes and electrons being more unbalanced. As a result, the $(fbi)_2Ir(acac)$ dopant can reduce the electron-hole balance and recombination, narrow the recombination zone and increase the charges/excitons accumulation at the interface of HTL/EML, leading to the reduction in EL efficiency and enhancement in efficiency roll-off [1c], as shown in table 1 and figure 2. And it is reasonable that the efficiency of W_2 is low and the color is unstable compared with W_1. On the other hand, since the $(MPPZ)_2Ir(acac)$ dopant has no influence on the holes transport but reduces the electron mobility, W_1 can exhibit relatively more balanced carriers than that of W_2, resulting in high efficiency, low efficiency roll-off and stable color [1c].

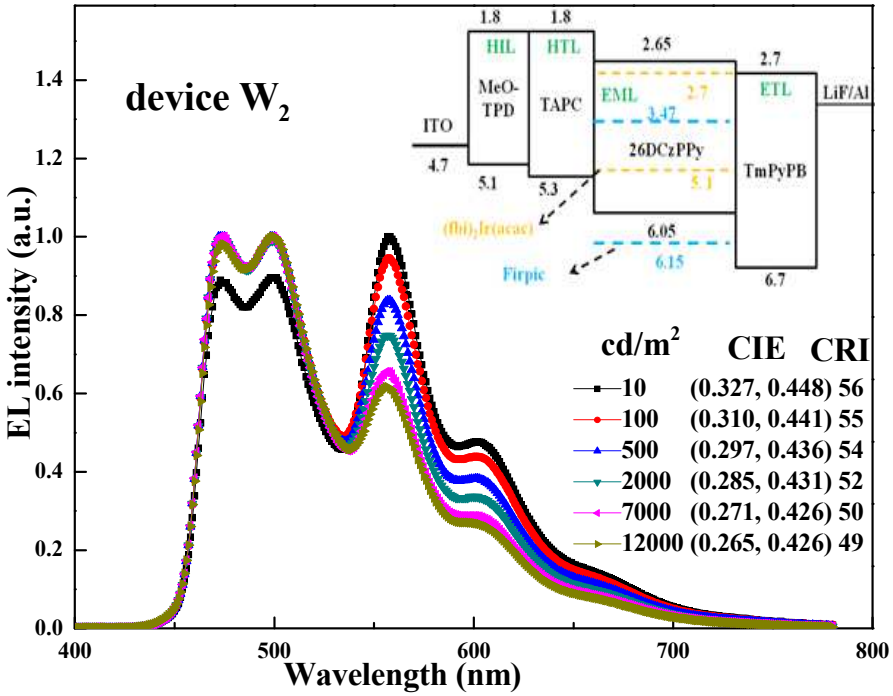

Figure. 5. Normalized EL spectra of W_2 at various luminances.

To confirm the above analysis that the unbalanced carriers can cause the poor efficiency as well as unstable color and to illustrate the key role of the bipolar host in the superior performances, two similar WOLEDs with the unipolar host of TAPC (W_3) or TmPyPB (W_4) were fabricated for comparison. The configurations are ITO/MeO-TPD : F4-TCNQ (100 nm, 4%)/TAPC (20 nm)/ hosts: Firpic : $(MPPZ)_2Ir(acac)$ (8 nm, 1: 25%: 1%)/TmPyPB (45 nm)/LiF (1 nm)/Al (200 nm), where hosts denote TAPC and TmPyPB for W_3 and W_4, respectively.

The spectra and efficiencies of the WOLEDs with unipolar hosts are given in figure 6a and figure 2, respectively. As shown in figure 6a, it is clearly found that both device W_3 and W_4 exhibit obvious variation of spectra. For example, the CIE coordinates variation of TAPC based device is (0.045, 0.015) in the range of luminance from 10 cd/m^2 to 6000 cd/m^2 and the variation of W_4 is (0.065, 0.023) from

10 cd/m^2 to 2000 cd/m^2. Moreover, both device W_3 and W_4 possess high efficiency roll-off compared with W_1, as depicted in figure 2 and table 1. These facts obviously demonstrate that the bipolar host shows more advantageous than the unipolar one to accomplish the trade-off of color-stability and efficiency roll-off in the single-EML WOLEDs. The reasons for these phenomena can be explained as follows.

As reported previously, the efficiency roll-off at high luminance/current density is mainly considered to result from TTA and triplet-polaron-quenching (TPQ) [17]. In the case of TTA, depending on the triplets density, the width of the exciton-formation zone within the EML has a great impact on the TTA and hence the efficiency roll-off. Owing to the high hole mobility and low electron mobility of TAPC host [10a, 10c], the exciton-formation zone of W_3 is located at the interface of EML/ETL, as vividly depicted in figure 6b. Whereas, due to the low hole mobility and high electron mobility of TmPyPB host [9], the exciton-formation zone of W_4 should be located at the interface of HTL/EML. As a result, narrow exciton-formation zones exist in W_3 and W_4. However, since 26DCzPPy host exhibits excellent bipolar transporting ability [7b], the exciton-formation zone of W_1 is expected to be distributed more uniformly within the EML instead of a narrow exciton-formation zone, avoiding the partially high triplet exciton density and thus suppressing the TTA [17], as vividly displayed in figure 6b. On the other hand, carriers and polarons accumulate at the interface and within the device active area, respectively, leading to TPQ [17b]. In this case, differences of energy levels as well as the carrier mobility between the EML and adjacent charge transporting layer (HTL or ETL) have a strong influence on the TPQ

and hence the efficiency roll-off. For device W_3, since the HOMO of TAPC (host) and TmPyPB (ETL) are 5.3 eV and 6.7 eV, respectively, holes are greatly accumulated at the interface of TAPC/TmPyPB due to the large energy barrier (1.4 eV). For device W_4, electrons are accumulated at the interface of TAPC/TmPyPB due to the significant LUMO difference between HTL and EML (0.9 eV). As a result, carriers are positioned at a shallow region of the EML/ETL (W_3) or HTL/EML (W_4) interface. However, due to the suitable energy levels between 26DCzPPy host and adjacent charge transporting layers (figure 1) together with the fact that 26DCzPPy exhibits high hole/electron mobility, both holes and electrons can effectively transport into the EML to recombine with each other rather than accumulate at the interface of HTL/EML or EML/ETL, leading to the suppression of TPQ. Therefore, both TTA and TPQ can be suppressed in W_1 by introducing the bipolar host, achieving reduced efficiency roll-off.

Since the use of the bipolar host which results in balanced charge fluxes and a broad distribution of recombination regions within the EML, the recombination ratio in the EML is expected to maintain invariant with increasing luminance, so as to keep the CIE coordinates almost constant [6b, 6f]. Therefore, the bipolar characteristic of 26DCzPPy host is beneficial to achieving such improved performances (stable color and low efficiency roll-off).

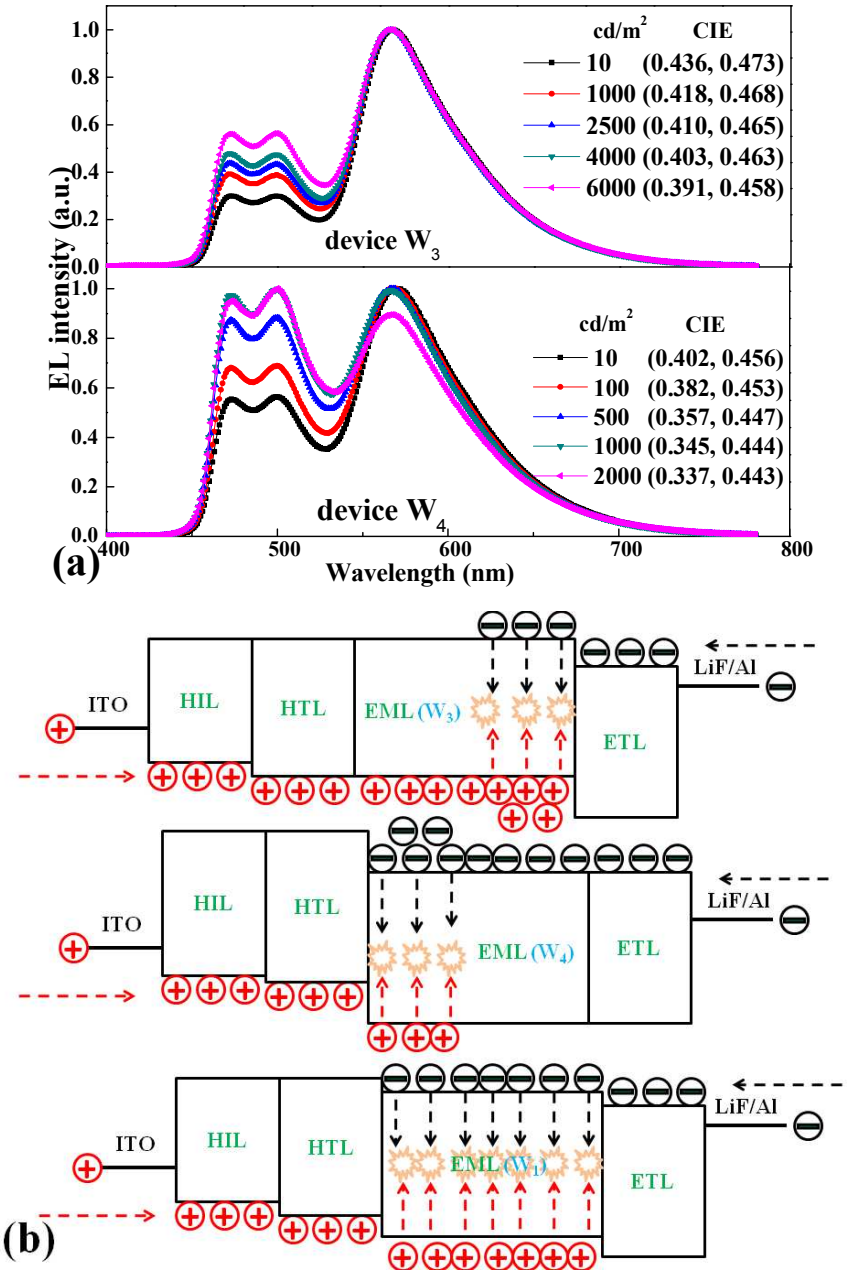

Figure. 6. (a) Normalized EL spectra of W_3 and W_4 at various luminances. (b) Diagrams of EL processes in device W_3, W_4 and W_1.

Table 1

Summary of device performances of the fabricated WOLEDs.

Device	$CE_{100/1000}$ [a] (cd/A)	$PE_{100/1000}$ [b] (lm/W)	L_{Max} [c] (cd/m^2)	CIE_{1000} [d]
W_1	45.2/43.6	37.1/31.3	34147	(0.385, 0.453)
W_2	37.6/35.4	25.2/20.6	23141	(0.292, 0.433)
W_3	34.4/31.0	30.9/23.2	12246	(0.418, 0.468)
W_4	20.8/9.5	18.2/6.2	2929	(0.345, 0.444)

[a]CE at 100 cd/m^2 and CE at a luminance of 1000 cd/m^2. [b] PE at 100 cd/m^2 and PE at 1000 cd/m^2. [c] Maximum luminance of the devices. [d] CIE coordinates of devices at 1000 cd/m^2.

4. Conclusion

In summary, we have demonstrated a highly efficient single-EML WOLED with low efficiency roll-off and stable color. The optimized device exhibits a forward-viewing CE of 45.2 cd/A at 100 cd/m^2 and slightly rolls off to 43.6 cd/A at 1000 cd/m^2. Moreover, a high forward-viewing PE of 31.3 lm/W is achieved at 1000 cd/m^2 and the color is very stable. The origin of the high performance is comprehensively investigated and an important phenomenon that the dopants with low concentrations have almost no effect on the electrical property when there are negligible energy barriers between the dopants and charge transport layers is demonstrated. Such presented results will provide guidelines to the rational design of both material and device structure for ultra high-performance WOLEDs. This contribution demonstrates that high efficiencies, low efficiency roll-off together with stable color can be simultaneously realized in simplified WOLEDs, which represents

a significant step towards the commercialization of WOLEDs in the emerging display and lighting applications.

AUTHOR INFORMATION

Corresponding Author

E-mail : zou1007@gmail.com (J. Zou); E-mail: psjbpeng@scut.edu.cn (J. Peng).

Acknowledgments

The authors are grateful to the National Natural Science Foundation of China (Grant Nos.61204087, 61306099), the Guangdong Natural Science Foundation (Grant No. S2012040007003), China Postdoctoral Science Foundation (2013M531841), the Fundamental Research Funds for the Central Universities (2014ZM0003, 2014ZM0034, 2014ZM0037, 2014ZZ0028) and the Specialized Research Fund for the Doctoral Program of Higher Education (Grant No. 20120172120008).

Reference

[1] (a) H. Sasabe and J. Kido, *J. Mater. Chem. C*, 2013, **1**, 1699.

(b) Lecamp, G. *SID Digest*, 2013, **43**, 597.

(c) Q. Wang and D. Ma, *Chem. Soc. Rev.*, 2010, **39**, 2387.

(d) Y. Tao, C. Yang and J. Qin, *Chem. Soc. Rev.*, 2011, **40**, 2943.

[2] H. Wu, G. Zhou, J. Zou, C. L. Ho, W. Y. Wong, W. Yang, J. Peng and Y. Cao, *Adv. Mater.*, 2009, **21**, 4181.

[3] (a) S. J. Su, E. Gonmori, H. Sasasbe and J. Kido, *Adv. Mater.*, 2008, **20**, 4189.

(b) Y. L.Chang, Y. Song, Z. Wang, M. G. Helander, J. Qiu, L. Chai, Z. Liu, G. D. Scholes and Z. Lu, *Adv. Funct. Mater.*, 2013, **23**, 705.

(c) H. Sasabe, J. Takamatsu, T. Motoyama, S. Watanabe, G. Wagenblast, N. Langer,

O. Molt, E. Fuchs, C. Lennartz, and J. Kido, *Adv. Mater.*, 2010, **22**, 5003.

(d) S. Reineke, F. Lindner, G. Schwartz, N. Seidler, K. Walzer, B. Lussem and K. Leo, *Nature*, 2009, **459**, 234.

[4] (a) X. H. Zhao, Z. S. Zhang, Y. Qian, M. D. Yi, L. H. Xie, C. P. Hu, G. H. Xie, H. Xu, C. M. Han, Y. Zhao and W. Huang, *J. Mater. Chem. C*, 2013, **1**, 3482.

(b) Y. S. Park, J. W. Kang, J. W. Park, Y. H. Kim, S. K. Kwon, and J. J. Kim, *Adv. Mater.*, 2008, **20**, 1957.

(c) E. Mondal, W. Y. Hung, H. C. Dai and K. T. Wong, *Adv. Funct. Mater.*, 2013, **23**, 3096.

(d) E. Mondal, W. Y. Hung, Y. H. Chen, M. H. Cheng and K. T. Wong, *Chem. Eur. J.*, 2013, **19**, 10563.

(e) C. Han, G. H. Xie, H. Xu, Z. Zhang, L. Xie, Y. Zhao. S. Liu and W. Huang, *Adv. Mater.*, 2011, **23**, 2491.

[5] (a) Q. Wang, J. Ding, D. Ma, Y. Cheng and L.Wang, *Appl. Phys. Lett.*, 2009, **94**, 103503.

(b) Q. Wang, J. Ding, D. Ma, Y. Cheng, L. Wang, X. Jing and F. Wang, *Adv. Funct. Mater.*, 2009, **19**, 84.

(c) W. Y. Huang, Z. W. Chen, H. W. You, F. C. Fan, H. F. Chen and K. T. Wong, *Org. Electron.*, 2011, **12**, 575.

(d) Y. H. Kim, K. W. Cheah and W. Y. Kim, *Appl. Phys. Lett.*, 2013, **103**, 053307.

[6] (a) C. L. Ho, L. C. Chi, W. Y. Hung, W. J. Chen, Y. C. Lin, H. Wu, E. Mondal, G. J. Zhou and W. Y. Wong, *J. Mater. Chem.*, 2012, **22**, 215.

(b) W. Y. Hung, G. M. Tu, S. W. Chen and Y. Chi, *J. Mater. Chem.*, 2012, **22**, 5410.

(c) S. Gong, Y. Chen, C. Yang, C. Zhong, J. Qin and D. Ma, *Adv. Mater.*, 2010, **22**, 5370.

(d) S. Gong, Y. Chen, J. Luo, C. Yang, C. Zhong, J. Qin and D. Ma, *Adv. Funct. Mater.*, 2011, **21**, 1168.

(e) X. Yang, H. Huang, B. Pan, M. P. Aldred, S. Zhuang, L. Wang, J. Chen and D. Ma, *J. Phys. Chem. C*, 2012, **116**, 15041.

(f) B. S. Kim and J. Y. Lee, *Org. Electron.*, 2013, **14**, 3024.

(g) H. Huang, X. Yang, B. Pan, L. Wang, J. Chen, D. Ma and C. Yang, *J. Mater. Chem.*, 2012, **22**, 13223.

(h) W. Y. Hung, L. C. Chi, W. J. Chen, E. Mondal. S. H. Chou, K. T. Wong and Y. Chi, *J. Mater. Chem.*, 2011, **21**, 19249.

(i) H. Huang, X. Yang, Y. Wang, B. Pan, L. Wang, J. Chen, D. Ma and C. Yang, *Org. Electron.*, 2013, **14**, 2573.

(j) B. Pan, B. Wang, Y. Wang, P. Xu, L. Wang, J. Chen and D. Ma, *J. Mater. Chem. C*, 2014, **2**, 2466.

(k) M. Zhu, J. Zou, S. Hu, C. Li, C. Yang, H. Wu, J. Qin and Y. Cao, *J. Mater. Chem.* 2012, **22**, 361.

[7] (a) S. J. Su, H. Sasabe, T. Takeda and J. Kido, *Chem. Mater.* 2008, **20**, 1691.

(b) C. Cai, S. J. Su, T. Chiba, H. Sasabe, Y. J. Pu, K. Nakayama and J. Kido, *Org. Electron.*, 2011, **12**, 843.

[8] G. Ge, J. He, H. Guo, F. Wang and D. Zou, *J. Organomet. Chem.,* 2009, **694**, 3050.

[9] S. J. Su, T. Chiba, T. Takeda and J. Kido, *Adv. Mater.*, 2008, **20**, 2125.

[10] (a) J. Lee, N. Chopra, S. H. Eom, Y. Zheng, J. Xue, F. So and J. Shi, *Appl. Phys. Lett.,* 2008, **93**, 123306.

[b] K. Goushi, R. Kwong, J. J. Brown, H. Sasabe and C. Adachi, *J. Appl. Phys.,* 2004, **95**, 7798.

[c] Y. Chen, F. Zhao, Y. Zhao, J. Chen and D. Ma, *Org. Electron.*, 2012, **13**, 2807.

[11] J. Zhou, N. Ai, L. Wang, H. Zheng, C. Luo, Z. Jiang, S. Yu, Y. Cao and J. Wang, *Org. Electron.*, 2011, **12**, 648.

[12] Y. Shao and Y. Yang, *Appl. Phys. Lett*., 2005, **86**, 073510.

[13] Q. Wang, C. L. Ho, Y. Zhao, D. Ma, W. Y. Wong and L. Wang, *Org. Electron.*, 2009, **11**, 238.

[14] M. T. Lee, H. H. Chen, C. H. Liao, C. H. Tsai and C. H. Chen, *Appl. Phys. Lett*., 2004, **85**, 3301.

[15] (a) F. Zhao, N. Sun, H. Zhang, J. Chen and D. Ma, *J. Appl. Phys.*, 2012, **112**, 084504.

(b) H. I. Baek and C. H. Lee, *J. Phys. D: Appl. Phys.*, 2008, **41**, 105101.

[16] (a) Y. S. Seo and D. G. Moon, *Synthetic Met.*, 2010, **160**, 113.

(b) P. S. Davids, I. H. Campbell and D. L. Smith, *J. Appl. Phys.*, 1997, **82**, 6319.

[17] (a) S. Reineke, K. Walzer and K. Leo, *Phys. Rev. B*, 2007, **75**, 125328.

(b) F. X. Zhang, T. C. Sum, A. C. H. Huan, T. L. Li, W. L. Li and F. Zhu, *Appl. Phys. Lett*., 2008, **93**, 023309.